Methods for Analytic Reflected Radiant Flux Modeling in Observing Space Vehicles

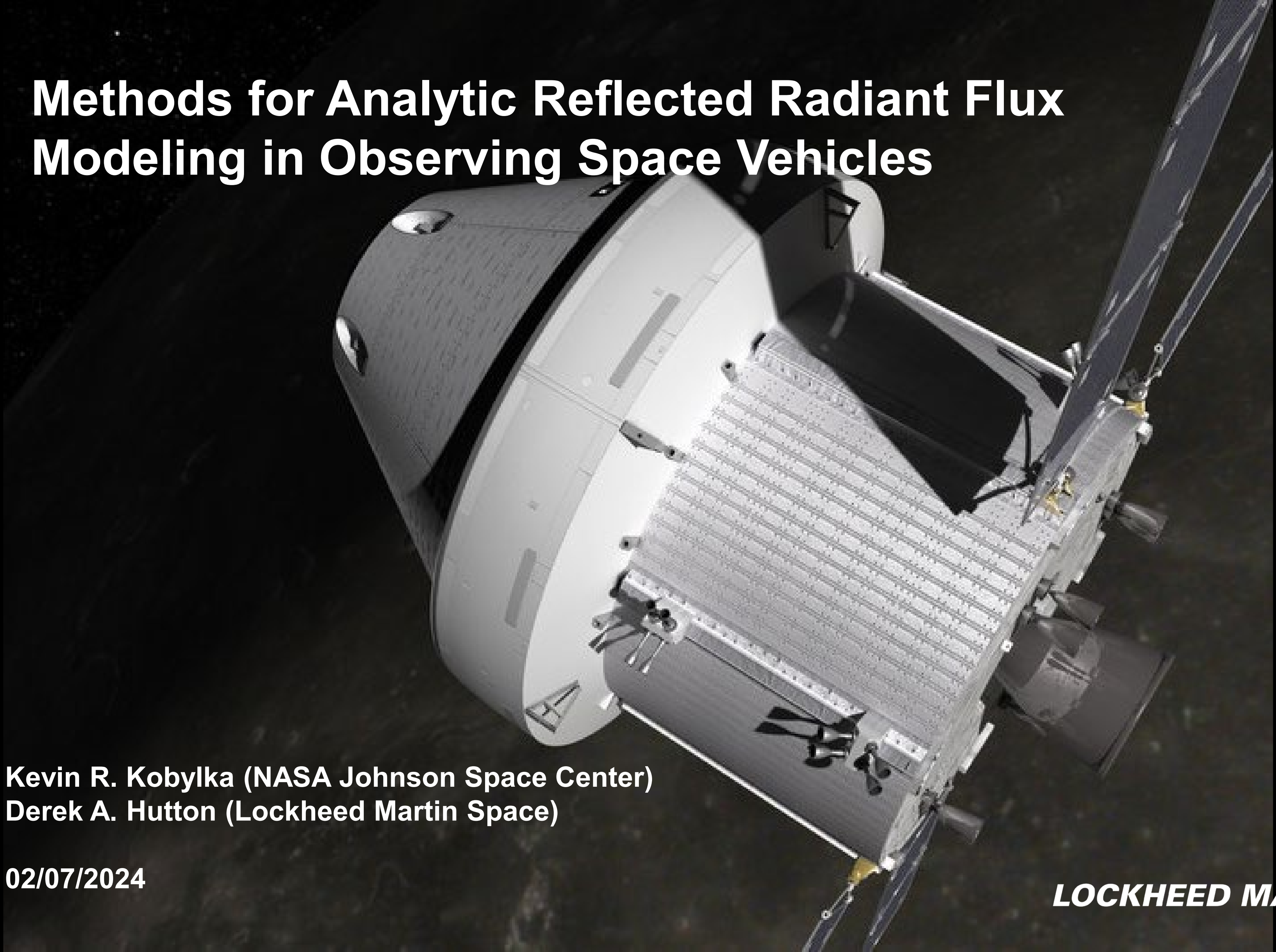

Kevin R. Kobylka (NASA Johnson Space Center)
Derek A. Hutton (Lockheed Martin Space)

02/07/2024

LOCKHEED MARTIN

Contents

- **Background**
  - Uses for Optical measurements in spacecraft navigation and space science
  - Optical Spacecraft Navigation systems on the Orion spacecraft
- **Artemis I Flight Test and Data Analysis**
  - Flight Test background
  - Predicted Brightness as a Function of Range
    - Analytic Brightness from Simplified Geometric Models
    - Analytic Brightness from Flat Surface Model
  - Mission Data Analysis
    - Image Processing Techniques and Results
    - Brightness Model Verification
    - Angular Rates
- **Conclusions and Forward Work**

Contents

- ♦ **Background**
  - Uses for Optical measurements in spacecraft navigation and space science
  - Optical Spacecraft Navigation systems on the Orion spacecraft
- ♦ **Artemis I Flight Test and Data Analysis**
  - Flight Test background
  - Predicted Brightness as a Function of Range
    - Analytic Brightness from Simplified Geometric Models
    - Analytic Brightness from Flat Surface Model
  - Mission Data Analysis
    - Image Processing Techniques and Results
    - Brightness Model Verification
    - Angular Rates
- ♦ **Conclusions and Forward Work**

Uses for Optical Measurements in Spacecraft Navigation

- **Optical Navigation** has been used for navigation relative to celestial bodies as well as in relative navigation between spacecraft.

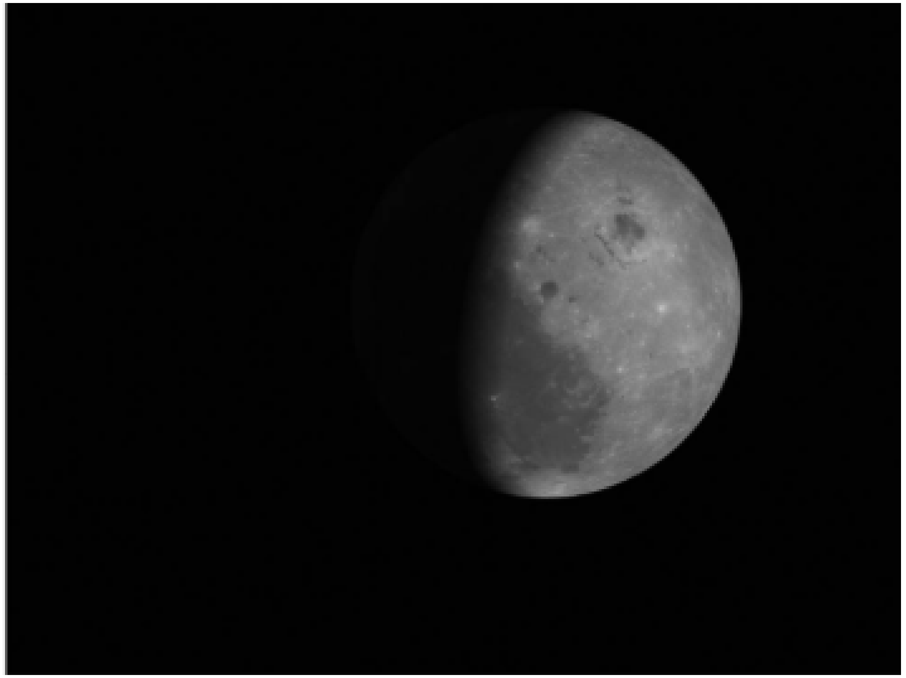

Image of Earth's Moon
Christian, J.A., "Accurate Planetary Limb Localization for Image-Based Spacecraft Navigation," Journal of Spacecraft and Rockets, Vol. 54, No. 3, 2017, pp 708-730.

Gemini VIII approaching Agena vehicle (photo credit: NASA)

Uses for Optical Measurements in Spacecraft Navigation

- Images gathered using a passive optical system can be used to generate a variety of measurements
- These are commonly **bearing measurements** to a target or features on a planetary surface and/or **range measurements** based on the size of a target in the image

Example of lit limb measurements

Example of bearing measurements to another vehicle

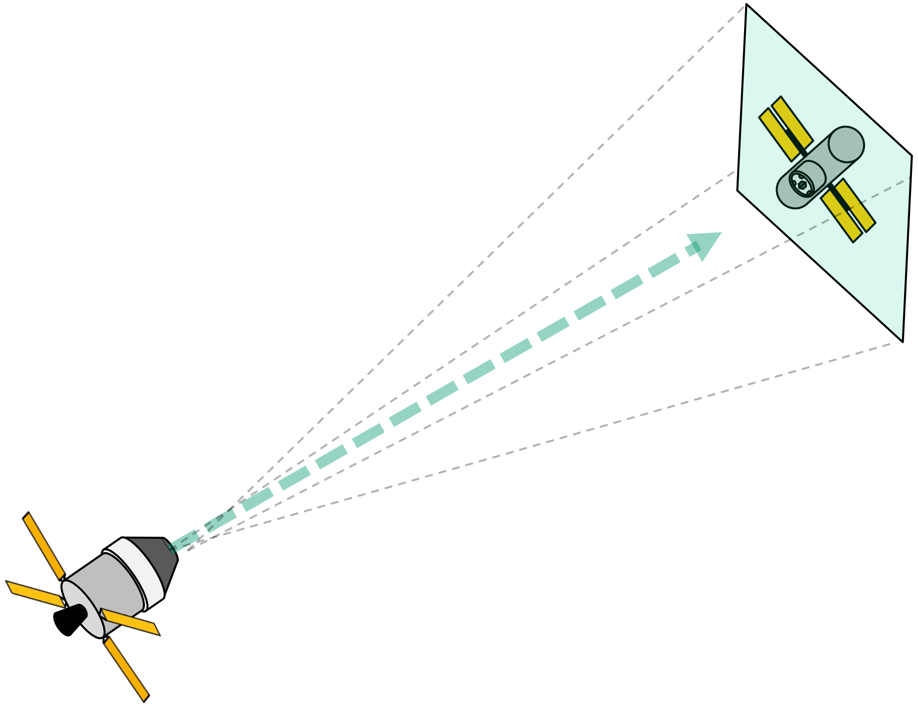

Christian, J.A., "Accurate Planetary Limb Localization for Image-Based Spacecraft Navigation," Journal of Spacecraft and Rockets, Vol. 54, No. 3, 2017, pp 708-730.

Optical Spacecraft Navigation systems on the Orion spacecraft

- The Orion spacecraft features two optical navigation systems

- The **OpNav Camera** is used to generate range and bearing measurements to the Earth/Moon to benefit absolute navigation

- The **Docking Camera** serves two purposes
  - The collection of **bearing measurements** to a target vehicle at long range during Rendezvous Proximity Operations and Docking (RPOD)
  - As a **piloting aid** at close range to estimate misalignment during the final phases of RPOD

Image of Earth obtained by the Orion Optical Navigation Camera (photo credit: NASA)

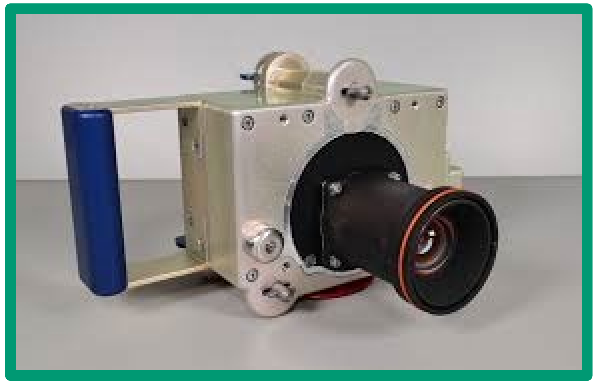

The Orion Docking Camera (photo credit: Malin Space Science Systems)

Contents

- Background
  - Uses for Optical measurements in spacecraft navigation and space science
  - Optical Spacecraft Navigation systems on the Orion spacecraft
- **Artemis I Flight Test and Data Analysis**
  - Flight Test background
  - Predicted Brightness as a Function of Range
    - Analytic Brightness from Simplified Geometric Models
    - Analytic Brightness from Flat Surface Model
  - Mission Data Analysis
    - Image Processing Techniques and Results
    - Brightness Model Verification
    - Angular Rates
- Conclusions and Forward Work

Flight Test Background

- The **Artemis I OpNav camera** has similar photodetector resolution and Field-Of-View as the **docking camera**
- The OpNav camera was used in a flight test to demonstrate **Long Range Bearing** similar to the docking camera use on future missions
- The upper stage of the SLS, the **Interim Cryogenic Propulsion Stage (ICPS)**, was imaged after separation at long range as a surrogate target vehicle
  - The fraction of incident light reflected by the different ICPS surfaces, albedo α, was estimated from pre-launch photographs

The Earth and Moon as seen by the Orion Spacecraft on Artemis I (photo credit: NASA)

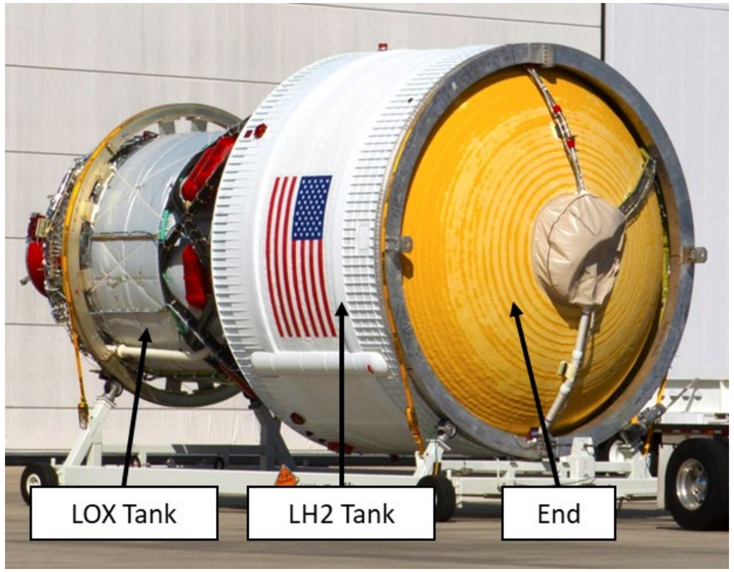

The Interim Cryogenic Propulsion Stage (ICPS) (photo credit: NASA)

Predicted brightness as a function of range:
Analytic Brightness from Simplified Geometric Models (1/2)

- At unresolved distances ICPS geometry can be approximated with **simplified geometric models**
- Applying Lambertian **Bidirectional Reflectance Distribution Function (BRDF)**, a reflected intensity as a function of illuminated projected area can be constructed
- Integrating reflected intensity gives the **total reflected brightness** $\bar{I}$

Side-on view of ICPS is modeled with a **cylinder**

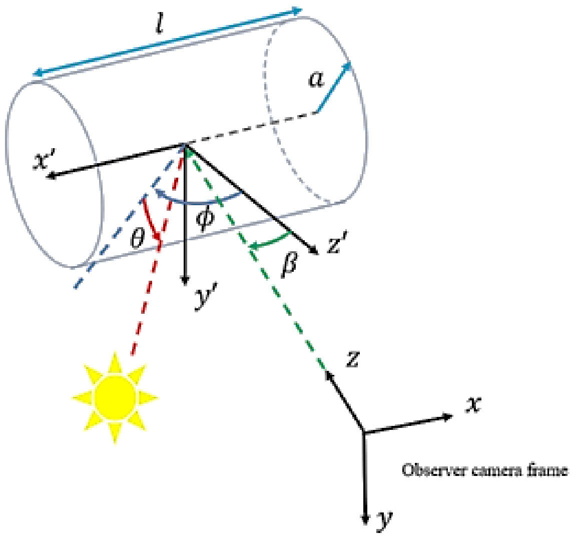

Cylinder total reflected brightness

$$\bar{I}_L^C = \frac{I_0 \alpha a l \cos(\beta)}{2}\left[\cos^2(\theta)\cos(\phi)\sin(\theta) + \cos(\theta)\cos(\phi)(\pi - \theta) + \sin^3(\theta)\right]$$

End-on view of ICPS is modeled with a **sphere**

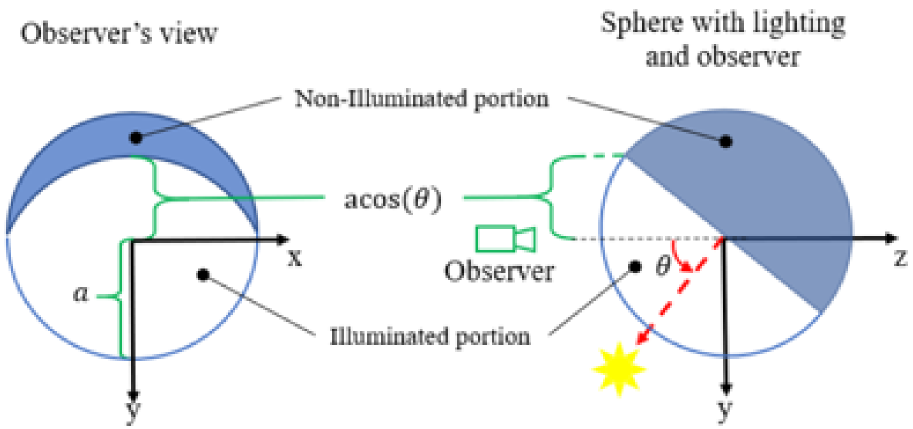

Sphere total reflected brightness

$$\bar{I}_L^S = \frac{2}{3} I_0 \alpha a^2 \left[\sin(\theta) + \cos(\theta)(\pi - \theta)\right]$$

Predicted brightness as a function of range:
Analytic Brightness from Simplified Geometric Models (2/2)

- **End-On View**
  - Modeled with a sphere at phase angles of 0 and 45 degrees

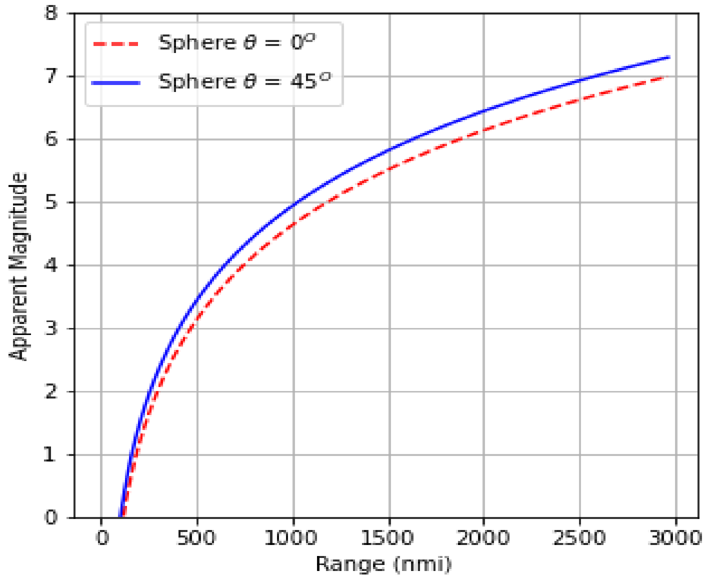

- **Side-On View**
  - Modeled with a cylinder at phase angles of 0 and 45 degrees
  - One large cylinder used to approximate body

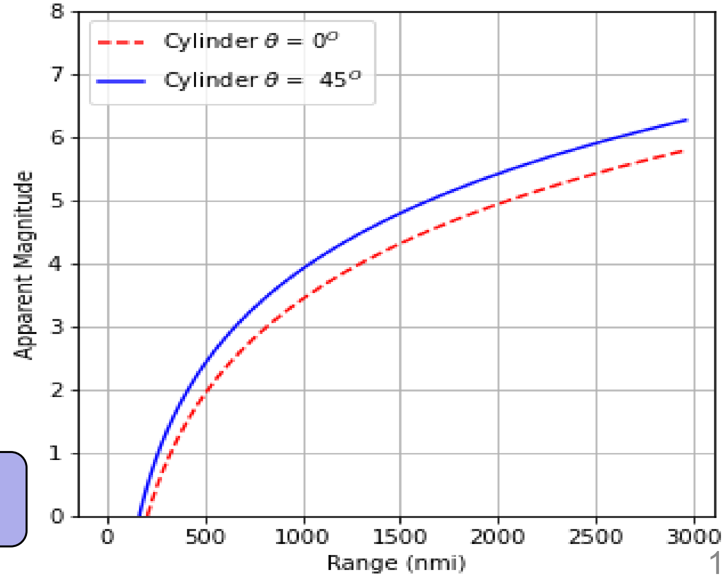

Simplified Geometric Model predicted magnitude of 5.5 – 7.0 at range of 2600 nmi.

Predicted brightness as a function of range:
Analytic Brightness using a flat surface model (1/2)

- Modeled ICPS as an **equivalent flat surface**
- **In-band Solar radiance** L_{sun} is Plank's blackbody radiation equation integrated over the camera waveband
- At 1 AU, the Sun subtends a cone with half angle of Θ_{sun} resulting in **Solar irradiance** reaching the reflecting surface of

$$E_{sun} = L_{sun} 4\pi \sin^2\left(\frac{\Theta_{sun}}{2}\right)$$

- **Irradiance received** at the camera after reflection from the Lambertian surface is

$$E_c = \frac{\alpha}{\pi} E_{sun} \cos\theta_{is} \frac{A}{d^2} \cos\theta_{ic}$$

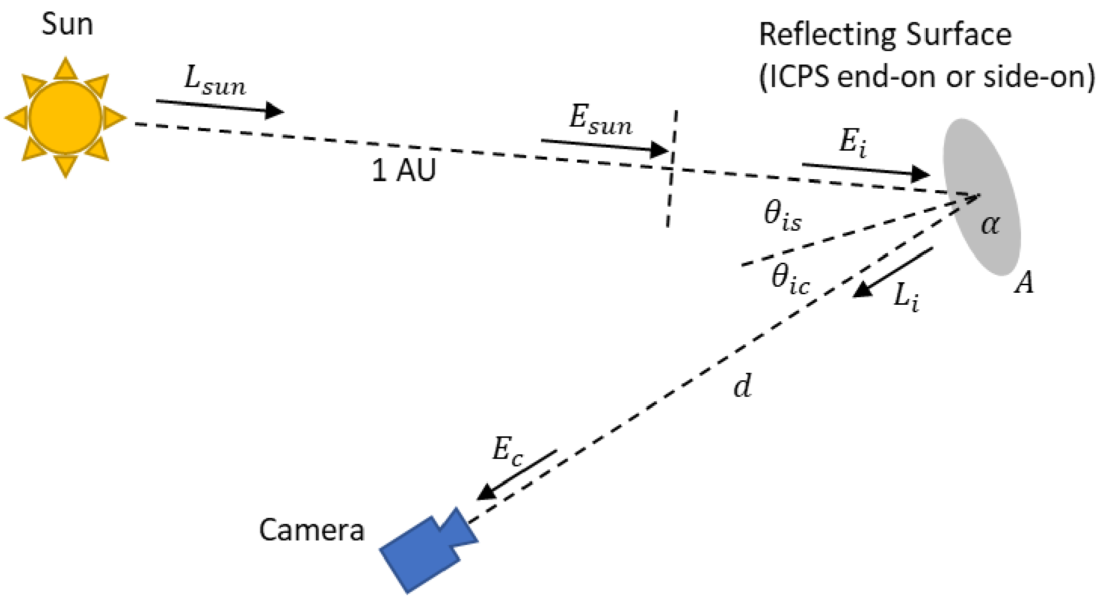

Predicted brightness as a function of range:
Analytic Brightness using a flat surface model (2/2)

End-On view

- Modeled end of LH2 tank as a **flat disk** and used radius of ICPS to compute the area

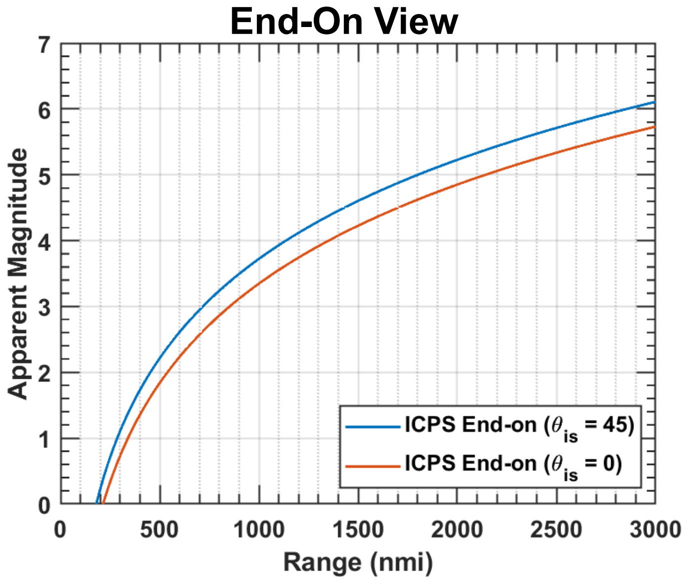

Side-On view

- Used **projected area** of each cylinder (length x diameter) **scaled by 0.5** to account for surface curvature
- Combined area of LOX and LH2 cylinders into a **single equivalent surface with constant albedo**
  - Scaled the area of the LOX surface based on the ratio of albedos

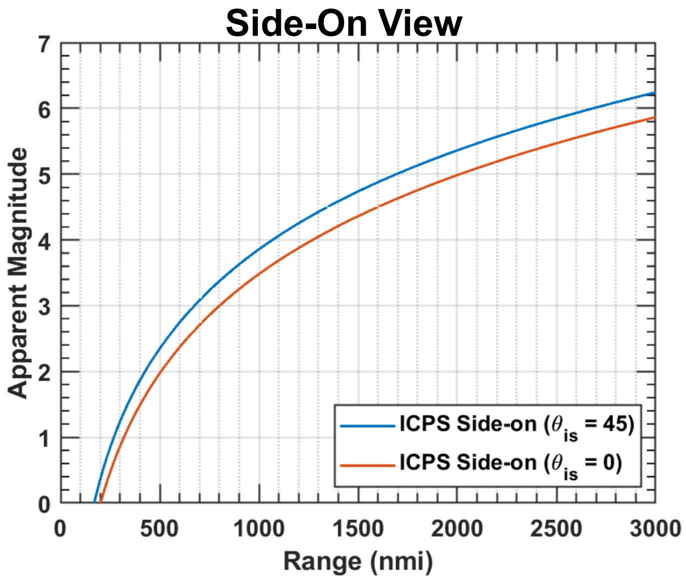

Flat Surface Model predicted magnitude of 5.5 – 6.0 at range of 2600 nmi.

- Several dozen images gathered with ICPS at range of approximately 2600 nautical miles
- Used COTS star ID and attitude determination tool
- Attitude estimated using ‘coarse’ star catalog with stars of apparent magnitude 5.5 and brighter
- Used ‘fine’ star catalog with magnitudes of 7.5 and brighter to reproject star locations
    - Filtered out centroids matching star locations, leaving only ICPS candidates

Full starfield of candidate centroids (blue x’s)
Mag >7.5 reprojected catalog stars (red o’s)

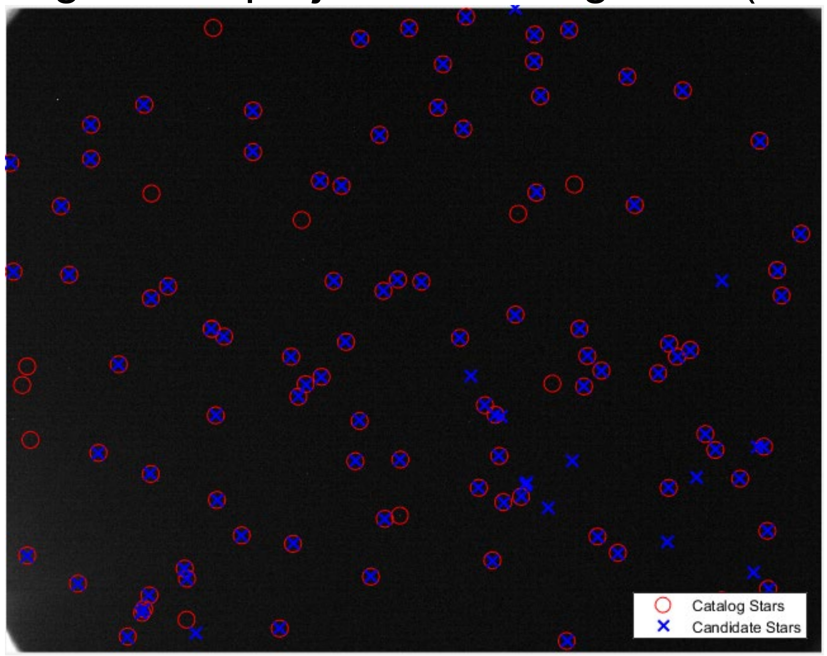

Filter using catalog

Remaining blue x’s are star-like non-stars

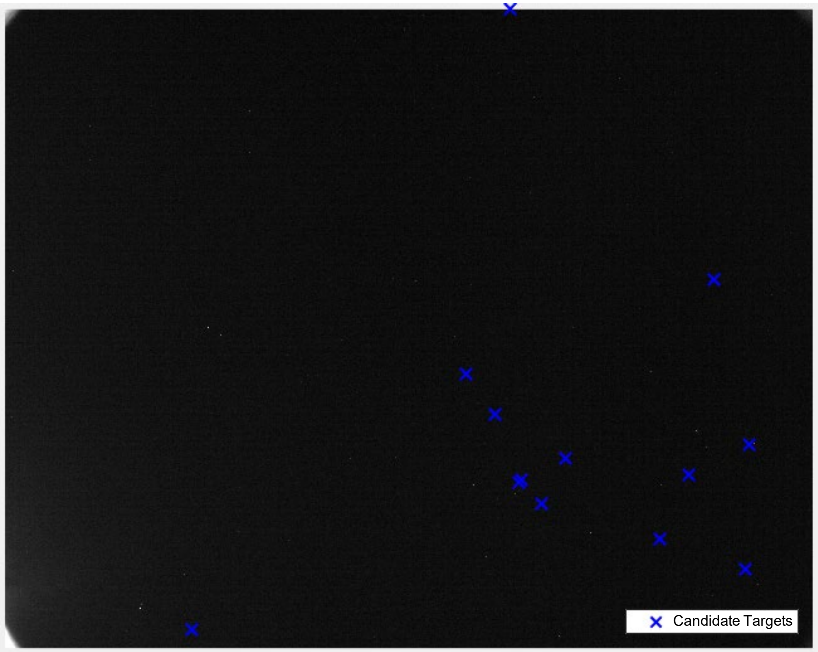

Image Processing Techniques and Results

- Expected ICPS image coordinates were determined using propagated trajectory information from the NASA Flight Dynamics Officers
  - Relative motion is negligible – ICPS expected to be stationary with respect to the star field
- Used centroid search with lowered thresholds in small region around expected location
- Consistent centroid detected a few pixels from the expected ICPS coordinates

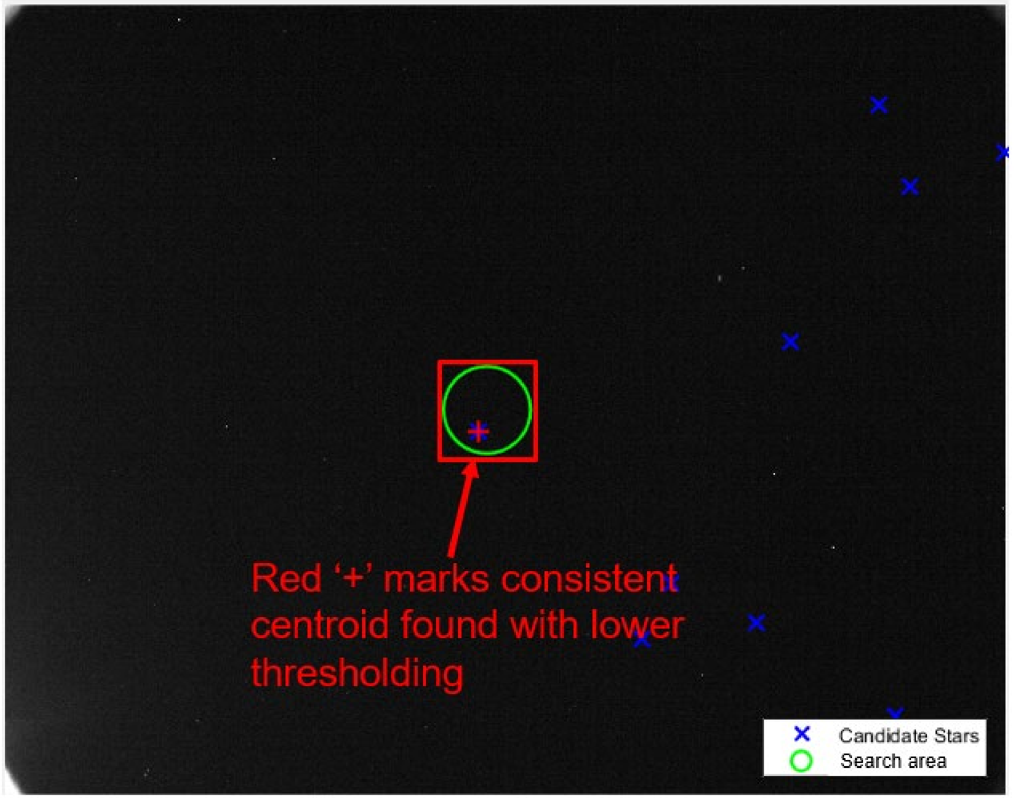

Image Processing Techniques and Results

- ICPS image was amplified by image stacking multiple frames – made possible due to small relative motion of ICPS

- Aligning and stacking windowed images revealed one extremely strong return in the expected ICPS location

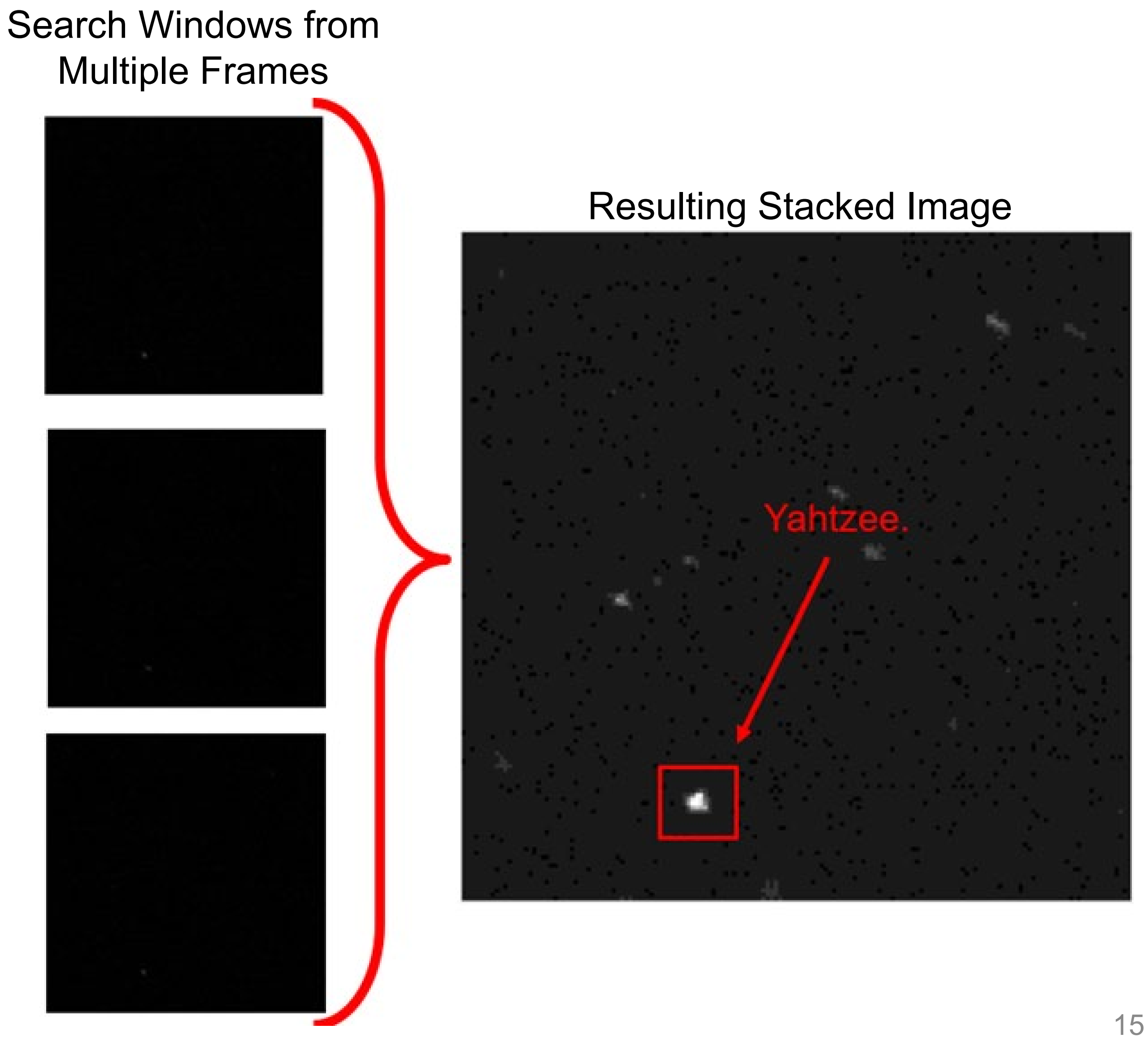

Brightness Model Verification

- The average peak pixel intensity for all ID'ed stars and the catalog apparent magnitude was recorded
- Logarithmic curve was fitted to image intensity and star magnitude data
- Fitted curve was used to estimate ICPS apparent magnitude based on the average peak pixel intensity of the ICPS centroids
  - The computed magnitude (~5.8) aligns well with preflight predictions from analytic models

Apparent Magnitude vs Centroid Pixel Intensity

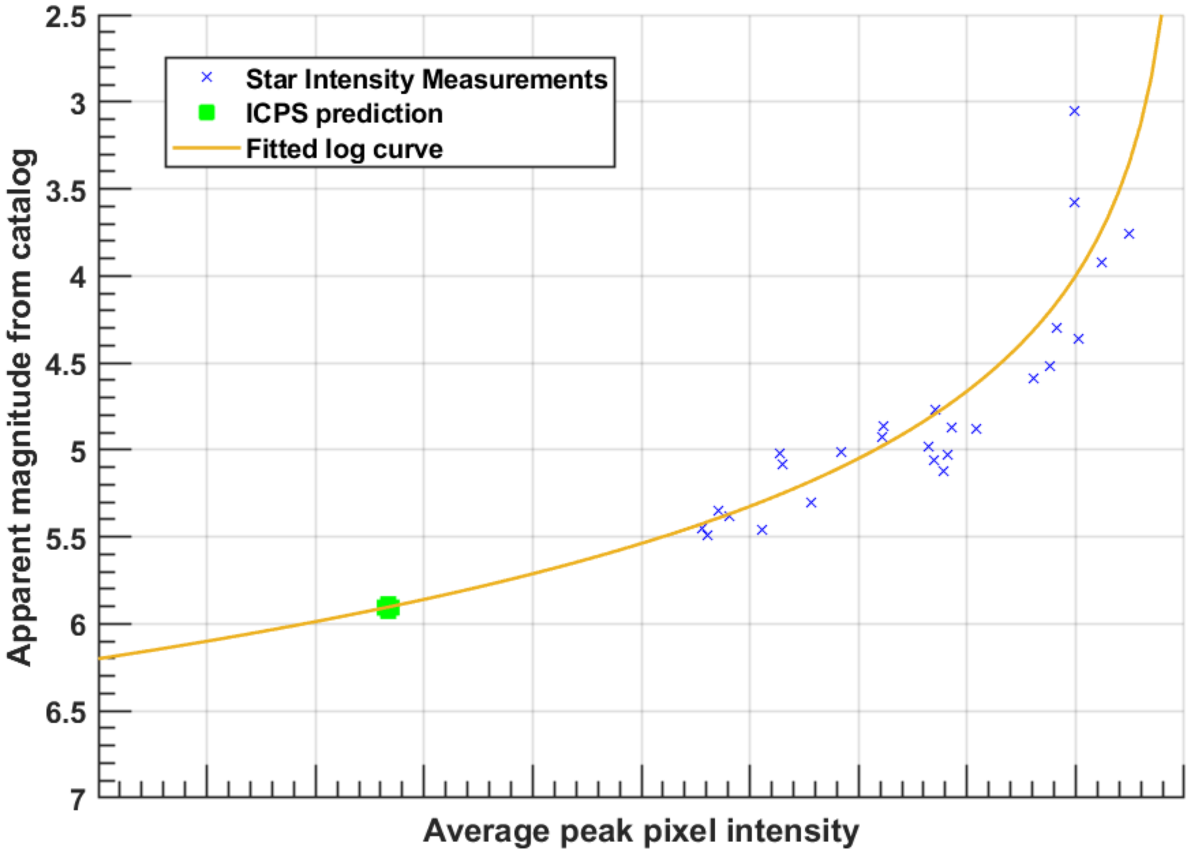

Angular Rates

- The peak pixel intensity of the ICPS centroid exhibited a periodic nature with both high and low frequency components
- This pattern is commonly seen in the intensity signatures of tumbling, oblong objects
- Peaks at several angular rates are visible when viewing the data in frequency space
  - Angular rates matched the expected ICPS tumble based on ICPS mass properties and maneuvers performed prior to loss-of-signal

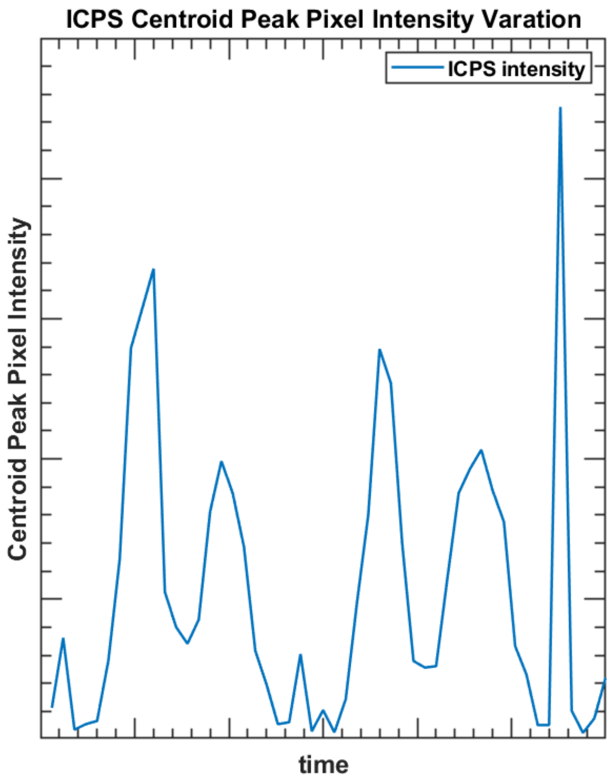

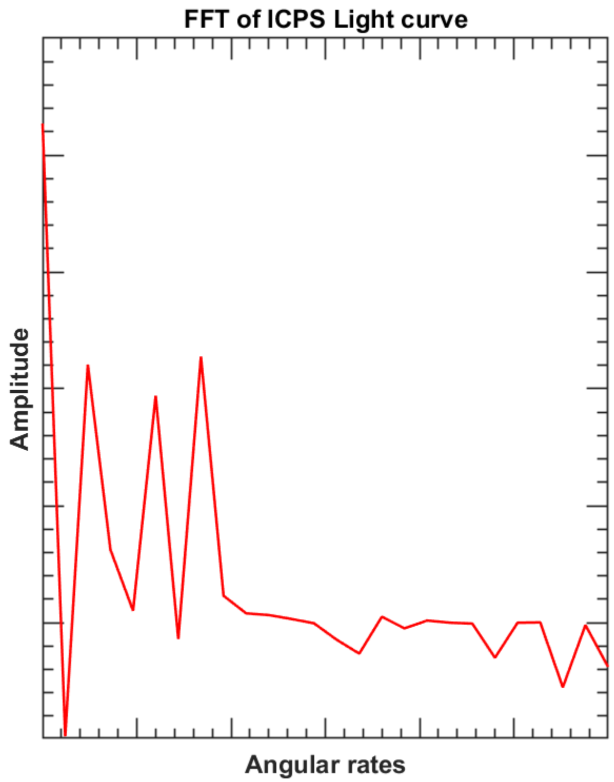

Contents

Conclusions and Forward Work

Conclusions

- Two analytic models for estimating apparent magnitude as a function of range for a target vehicle developed
- Flight data from Artemis I Flight Test validated model predictions
- Builds confidence in using a similar analysis for future missions to predict target vehicle brightness as a function of range during RPOD activities
  - This will aid in informing planned camera settings preflight
- Post-flight analysis demonstrated that, while star subtraction alone was insufficient at these ranges, more intricate techniques can still be used to generate bearing measurements at very long range
  - In addition, attitude rate information on the target vehicle can be determined
  - Demonstrates the still untapped potential optical systems have in these applications

Forward work

- Further development of models – combining the strengths of the two models presented here
- Testing with Artemis II docking camera flight data